

The integral in Eq. (7) will then read

$$\left[\frac{u_i(x) - u_\infty}{u_\infty} \right]^2 \int_{\xi=0}^1 E(|x - \xi|; r) d\xi = \frac{1}{\pi} \left(\frac{u_i(x) - u_\infty}{u_\infty} \right)^2 \left\{ r^{-1} \ln(1 + r^2) + 2 \arctan r^{-1} + (1 + r^{-2}) \arctan r - r^{-1} - \frac{\pi}{2} \right\}$$

or be written in a series form,

$$\left[\frac{u_i(x) - u_\infty}{u_\infty} \right]^2 \int_{\xi=0}^1 E(|x - \xi|; r) d\xi = \frac{1}{\pi} \left(\frac{u_i(x) - u_\infty}{u_\infty} \right)^2 \left\{ \frac{\pi}{2} - \frac{1}{3} r + \frac{1}{30} r^3 - \dots \right\} \quad (r < 1) \quad (9)$$

Equation (9), with the first two terms retained in the series expansion, is substituted back in Eq. (7) and one obtains the desired result,

$$\frac{u(x) - u_\infty}{u_\infty} = \frac{1}{\beta} \left[\frac{u_i(x) - u_\infty}{u_\infty} \right] + \frac{3\pi + 2r}{12\pi(1 - M_\infty^2)(1/M_\infty^* - 1)} \left[\frac{u_i(x) - u_\infty}{u_\infty} \right]^2 \quad (10)$$

Here $r = r(x)$ is determined from Eq. (6) and the value for the pressure coefficient c_p can again be found from Eq. (8).

The compressibility rule described by Eq. (10) will be tested on a symmetrical blunt-nosed airfoil. The exact pressure distribution for this airfoil at nearly critical freestream Mach number is given in Ref. 11 together with geometric profile data. These again have been utilized to calculate the incompressible solution by using a mapping method which is briefly described in Ref. 12. Various compressibility corrections were applied to the incompressible values, and the obtained results are plotted together with the exact values in Fig. 1. It can be seen that none of the applied correction formulas can satisfactorily account for the global change of the pressure distribution with increasing freestream Mach number. This is not surprising since the correction factors are constants based on the freestream condition only. For a discussion of introducing the profile surface slope into the correction factors, the reader is referred to the work of Wilby.¹³

In Fig. 2 the result of the present analysis as applied to the same airfoil problem of Fig. 1 is given. Due to the additional dependence on profile curvature (see Fig. 3), the compressibility correction defined by Eq. (10) yields reduced corrections to the Prandtl-Glauert value at locations of large curvature, e.g., at the nose region. This is the essential feature of the present approach and it is viewed as an improvement over other correction methods.

References

¹ Tsien, H., "Two-Dimensional Subsonic Flow of Compressible Fluids," *Journal of the Aeronautical Sciences*, Vol. 6, No. 10, Aug. 1939, pp. 399-407.

² Ringleb, F., "Näherungsweise Bestimmung der Druckverteilung einer adiabatischen Gasströmung," FB 1284, 1940, Zentrale für wissenschaftliches Berichtswesen der Luftfahrtforschung des Generalluftzeugmeisters (ZWB), Berlin.

³ Temple, G. and Yarwood, J., "The Approximate Solution of the Hodograph Equations for Compressible Flow," Rept. S.M.E. 3201, June 1942, British Royal Aircraft Establishment, Farnborough, England.

⁴ Garrick, I. E. and Kaplan, C., "On the flow of a compressible fluid by the hodograph method. I—Unification and extension of present-day results," Rept. 789, Jan. 1944, NACA.

⁵ Krahn, E., "Näherungsverfahren zur Berechnung kompressibler Unterschallströmung," *Zeitschrift für Angewandte Mathematik und Mechanik*, Band 29, Heft 1/2, Jan./Feb. 1949, pp. 2-3.

⁶ Laitone, E. V., "New Compressibility Correction for Two-

Dimensional Subsonic Flow," *Journal of the Aeronautical Sciences*, Vol. 18, No. 5, May 1951, p. 350.

⁷ Van Dyke, M. D., "The Second-Order Compressibility Rule for Airfoils," *Journal of the Aeronautical Sciences*, Vol. 21, No. 9, Sept. 1954, pp. 647-648.

⁸ Imai, I., "The Second-Order Thin Airfoil Theory for Compressible Flow," *Journal of the Aeronautical Sciences*, Vol. 22, No. 4, April 1955, pp. 270-271.

⁹ Panchenkov, A. N., "Nesushchaya Poverkhnost' v Okolozvukovom Potokе Gaza," edited by I. L. Rozovskii, Gidrodinamika Bolshikh Skorostei, Izdatelstvo Naukova Dumka, Kiev, 1967, pp. 7-20 (English translation available from SLA as 68-12561-01A).

¹⁰ Nörstrud, H., "Numerische Lösungen von schallnahen Strömungen um ebene Profile," Ph.D. thesis, June 1968, Vienna Institute of Technology, Austria.

¹¹ Boerstoel, J. W., "Symmetrical subsonic potential flows around quasi-elliptical aerofoil sections," NRL TR 68016, 1968, National Aerospace Laboratory, Amsterdam, Holland.

¹² Asaka, S. and Hayasi, N., "An improved thin-airfoil theory for an arbitrary airfoil in a subsonic flow," ER-8979, March 1969, Lockheed-Georgia Research, Marietta, Ga.

¹³ Wilby, P. G., "The Calculation of Sub-Critical Pressure Distributions on Symmetric Aerofoils at Zero Incidence," NPL Aero Rept. 1208, March 1967, National Physical Laboratory, Teddington, England.

Rapid Calculation of Inviscid and Viscous Flow over Arbitrary Shaped Bodies

H. A. DWYER,* E. D. DOSS,† and A. GOLDMAN†
University of California, Davis, Calif.

Introduction

THE purpose of this Note is to show how the high Reynolds number viscous and inviscid flow over arbitrary shaped two-dimensional bodies, and in particular airfoils, can be calculated very rapidly and exactly with a modern digital computer. The calculations will only be carried out for the high Reynolds number case, so that the boundary layer and potential flow approximations can be made. (This of course, restricts the viscous flow calculation to a region of flow in front of the separation point.) Also, the results presented in this paper will be limited to incompressible flow and laminar flow in the boundary layer; although turbulent flow calculations have been carried out.

The basic methods which are employed in the paper are the following: 1) a numerical solution of the potential flow equations by a general method developed by Theodorsen and Garrick,¹ and 2) finite difference solution^{2,3} of the boundary-layer equations near the body surface up to the point of flow separation. These two methods were combined into one computer program which calculated the potential and boundary-layer flow over the body in a matter of seconds on the digital computer. The input for this program consisted solely of the body coordinates, angle of attack or net circulation, and the fluid properties. (For the purpose of illustration the calculation technique was applied to the flow over a NACA 0012 airfoil section.)

One of the main reasons for writing this Note is to point out the power of the digital computer in solving these types of difficult flow problems. As will be shown in the following, the methods used are more exact and less time consuming than all of the approximate techniques still employed in design and

Received July 22, 1970.

* Associate Professor, Mechanical Engineering Department.
Member AIAA.

† Research Assistant.

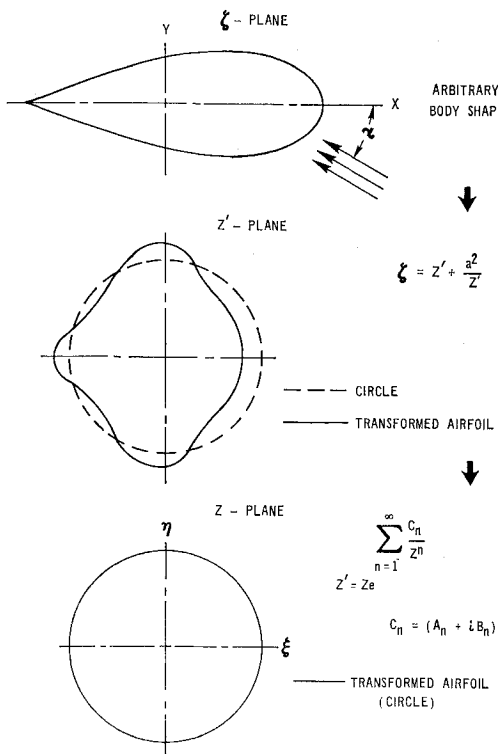


Fig. 1 Theodorsen transformation.

taught in fluid mechanics courses (such as linearized potential flow techniques⁴ and integral boundary-layer⁵ analyses). Also, if a small amount of time is spent in printing out the results of the calculations cleverly, enormous physical insight can be obtained by having the computer calculate the ratio to the various terms in the momentum equation at various parts of the boundary layer. For example, direct verification of both the potential and boundary-layer flow approximations can be readily obtained.

Methods of Approach

As mentioned previously the incompressible potential flow outside of the boundary layer will be calculated by the use of the theory developed by Theodorsen.¹ This theory is based mainly on the methods of complex variables and conformal mapping and has proven to provide exact and accurate results. It has been applied successfully to arbitrary bodies, and it lends itself to direct numerical solution. The basic idea behind the method is to transform an arbitrary body into a circle. (Theodorsen,¹ i.e., shows how a square can be readily transformed into a circle.) Since the potential flow over a circle is known for the cases of zero and finite circulation, all that is required to solve the arbitrary body problem is to transform back to the physical plane. A listing of the major conformal mappings and their effects are presented in Fig. 1. The actual solution of the problem reduces to a compact integral equation which can be solved by a direct numerical process. The numerical process used in this paper was similar to that in Ref. 1, however, the calculations were carried out with a digital computer, instead of graphically.

With the potential flow found by the procedure listed above, the boundary-layer flow can be calculated. The method of solution of the boundary-layer equations was an implicit-difference scheme of the Crank-Nicolson type^{2,3} for the laminar flow case and a full implicit scheme⁶ for the turbulent boundary-layer flow. The incompressible boundary-layer flow equations are given below:

$$\partial u / \partial x + \partial v / \partial y = 0 \quad (1)$$

$$u \partial u / \partial x + v \partial u / \partial y = -(1/\rho) \partial p / \partial x + v \partial^2 u / \partial y^2 \quad (2)$$

where u and v are the boundary layer velocities in the x and y directions, respectively. (The x coordinate is measured parallel to the wall and the y coordinate normal.)

The boundary-layer problem can be considerably simplified by transforming the dependent and independent variables. The object of the transformations are the following: 1) limit boundary layer growth and locate approximately the edge of the boundary layer a priori, 2) decrease velocity gradients in both coordinate directions, and 3) remove leading edge singularities and starting difficulties. The transformations which were used are

$$f' = u/u_e \quad \xi = x \quad \eta = y(u_e/2\nu x)^{1/2}$$

where u_e = inviscid surface velocity. The resulting form of the transformed boundary-layer equations are as follows: continuity

$$\xi \partial f' / \partial \xi + (\partial f' / \partial \eta)(\eta/2)(\beta_x - 1) +$$

$$\partial V / \partial \eta + \beta_x f' = 0 \quad (3)$$

momentum

$$\xi f' \partial f' / \partial \xi + \bar{V} \partial f / \partial \eta = \beta_x (1 - f'^2) + \frac{1}{2} \partial^2 f' / \partial \eta^2 \quad (4)$$

where

$$\beta_x = (\xi/u_e) \partial u_e / \partial \xi \quad V = v(x/2\nu u_e)^{1/2}$$

$$\bar{V} = V + f'(\eta/2)(\beta_x - 1)$$

In this transformed coordinate system the boundary-layer profiles change mainly as a result of changes in pressure. Therefore, the number of steps chosen to be taken in the x direction can be obtained from the inviscid flowfield. This usually means that the location of the x grid points correspond with those obtained from the inviscid flow calculation, and this simplifies the coupling of the two programs together. The boundary conditions for Eqs. (3) and (4) are

$$\eta = 0 \quad f' = 0 \quad V = 0$$

$$\eta = \infty \simeq 6 \quad f' = 1.0 \quad (-1/\rho) \partial p / \partial x = u_e \partial u_e / \partial x$$

The choice of $\eta = 6$ as the outer edge of the boundary layer in laminar flow has been found to be satisfactory for all problems treated, and can be changed to a larger value, if necessary.

The transformations do not change the characteristics of the finite difference methods, and the same stability and convergence behavior is obtained in the physical or transformed plane. A detailed listing of the Eqs. (3) and (4) in finite-difference form can be found in Ref. 2 and 3.

Calculations and Results

In order to illustrate the power of the two calculation techniques, the potential and incompressible, laminar boundary-layer flow over a NACA 0012 airfoil section⁷ has been inves-

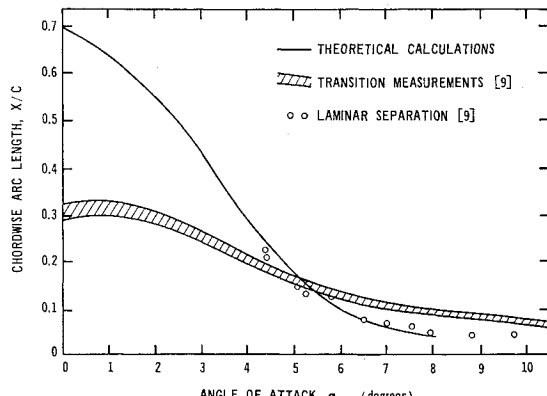


Fig. 2 Laminar separation on a NACA 0012 airfoil.

tigated for various angles of attack. The potential flow program required only the shape of the NACA 0012 section and the angle of attack to carry out the calculation. On the average a typical calculation was carried out for 80 points around the airfoil section surface, and required only two seconds of computer time on an IBM 7044 digital computer. All of the velocity and pressure calculations agreed with 2% or better of those presented in Ref. 8. The small discrepancy could be due to the fact that the present method probably used more points on the airfoil surface in the calculations. With these results it is seen that a digital computer can truly make Theodorsen's technique a useful and practical everyday design technique.

With the inviscid velocity and pressure calculated from the potential flow, the boundary-layer flow can be computed. The boundary-layer calculation starts at the stagnation point and proceeds step by step in the x direction until the point of separation (separation is defined as the point where u first becomes negative) is reached, after which it is impossible to proceed further with Eqs. (3) and (4). The results of these calculations are shown in Fig. 2 where the laminar separation point on the upper surface of the NACA 0012 airfoil section has been computed as a function of the angle of attack. The ordinate of the graph is the cordwise distance from the zero angle-of-attack stagnation point, whereas the abscissa is the local angle of attack.

For angles of attack less than 4° or 5° it can be seen from Fig. 2 that the laminar flow calculations are academic, since transition occurs on the airfoil section before laminar separation. However, for angles of attack equal to 50 or greater, laminar separation occurs before transition. Actually, the laminar separation causes the formation of a separation bubble, which plays a significant role in transition and turbulent boundary-layer reattachment. In Ref. 9 measurements on the location of the laminar separation bubble were presented, and it is seen from Fig. 2 that agreement between the theoretical calculations and experiments is excellent. The average boundary-layer calculation took four seconds of computer time on an IBM 7044 computer, and the step size in the η direction was $\Delta\eta = 0.1$. (This corresponds to sixty points across the boundary layer for $\eta \rightarrow \infty \simeq 6.0$.) The step size in the x direction was made variable, so that small steps were taken in regions of large pressure variations and large steps in regions of small pressure variation. Also, the experimental location of the laminar separation point should not be sensitive to Reynold's number since the mechanisms for the causation of both the separation bubble and turbulent reattachment are basically inviscid.

Summary and Conclusions

From the previous calculations it was shown that the inviscid flow, pressure distribution and boundary layer flow can be calculated exactly and rapidly over typical airfoil sections. The calculations involve only seconds of computer time on an IBM 7044 computer (not large by current standards), and are capable of giving as much detail as desired about the flowfield. Also, the calculation procedures presented are applicable to arbitrary shaped bodies, and their validity is limited only by the validity of the potential and boundary-layer approximations themselves. Because of the large scale availability of digital computer facilities throughout the world, techniques of calculation like those presented in this paper should have a great impact on the teaching of aerodynamics and on the use of theory in design procedures.

References

- 1 Theodorsen, T. and Garrick, I. E., "General Potential Theory of Arbitrary Wing Sections," TR 452, 1933, NACA.
- 2 Blottner, F., "Finite Difference Methods of Solution of the Boundary-Layer Equations," *AIAA Journal*, Vol. 8, No. 2, Feb. 1970, pp. 193-205.

³ Dwyer, H. A., "Solution of a Three-Dimensional Boundary-Layer Flow with Separation," *AIAA Journal*, Vol. 6, No. 7, July 1968, pp. 1336-1342.

⁴ Thwaites, B., *Incompressible Aerodynamics*, Oxford University Press, New York, 1960.

⁵ Schlichting, H., *Boundary Layer Theory*, 6th ed., McGraw-Hill, New York, 1968.

⁶ Richtmyer, R. D. and Morton, K. W., *Difference Methods for Initial Value Problems*, Interscience Publishers, New York, 1st ed., 1957, 2nd ed., 1967.

⁷ Von Mises, R., *Theory of Flight*, Dover, New York, 1959.

⁸ Abbott, I. H. and von Doenhoff, A. E., *Theory of Wing Sections*, McGraw-Hill, New York, 1949.

⁹ McCroskey, W. J. and Dwyer, H. A., "Methods of Analyzing Propeller and Rotor Boundary Layers with Crossflow," *Symposium on Analytical Methods in Aircraft Aerodynamics*, NASA, Oct. 1969.

Ratio of Turbulent Flight Miles to Total Flight Miles in the Altitude Range 45,000-65,000 ft

EDWARD V. ASHBURN* AND DAVID E. WACO†
Lockheed-California Company, Burbank, Calif.

Introduction

WHEN an aircraft that is flying through a portion of the atmosphere in which there are no clouds undergoes accelerations that cannot be directly attributable to the movement or setting of the control surfaces or to the flight characteristics of the aircraft, the aircraft is said to be in clear air turbulence. The accelerations of the aircraft are functions of the weight and characteristics of the aircraft in addition to the atmospheric gusts. If the ratio of the turbulent flight miles to total flight miles is to be computed, definitions of turbulent and total flight miles are required. The definition of the turbulent flight miles must include statements that give 1) the lower limit of accelerations that are considered to be turbulence, 2) the frequency interval of interest, and 3) a quantitative evaluation of the duration of turbulence. The ratio may also be a function of 1) the distribution of the total flight miles by season, altitude and underlying terrain, 2) the use and relative success of turbulence search or avoidance procedures, and 3) pattern flying through a known turbulent region.

Discussion and Results

In the High Altitude Clear Air Turbulence (HICAT) program, Crooks, Hoblit, and Prophet¹ defined turbulence as existing if rapid e.g. accelerations in excess of $\pm 0.10 g$ were observed for a duration of at least 10 sec. In his review of the VGH data from 768,000 miles in the altitude range 40,000-70,000 ft, Steiner² defined turbulence to exist "whenever the accelerometer trace was disturbed and contained gust velocities (presumably 'derived' gust velocities) greater than 2 fps." A comparison of the HICAT derived gust velocities with those given by Steiner indicates that the two definitions are roughly equivalent. Crooks et al.,¹ and Ashburn, Waco, and Melvin³ also defined turbulence in terms of the rms gust velocity. This definition is not useful for determining the ratio of turbulent flight miles to total flight miles because the rms gust velocity data are not available for all the turbulent regions observed.

Received September 8, 1970.

This work was supported by AFFDL under Contract F33615-69-C-1552.

* Head, Atmospheric Physics Laboratory.

† Research Meteorologist, Atmospheric Physics Laboratory.